J Neurosurg 106:660–666, 2007

Correlation of magnetic resonance spectroscopic and growth characteristics within Grades II and III gliomas

Tracy R. McKnight, Ph.D.,[1] Kathleen R. Lamborn, Ph.D.,[2] Tonya D. Love, B.S.,[2] Mitchel S. Berger, M.D.,[2] Susan Chang, M.D.,[2] William P. Dillon, M.D.,[1] Andrew Bollen, M.D.,[3] and Sarah J. Nelson, Dr. rer. nat.[1]

Departments of [1]Radiology, [2]Neurological Surgery, and [3]Pathology, University of California, San Francisco, California

Object. The accurate diagnosis of World Health Organization Grades II and III gliomas is crucial for the effective treatment of patients with such lesions. Increased cell density and mitotic activity are histological features that distinguish Grade III from Grade II gliomas. Because increased cellular proliferation and density both contribute to the in vivo magnetic resonance (MR) spectroscopic peak corresponding to choline-containing compounds (Cho), the authors hypothesized that multivoxel MR spectroscopy might help identify the tumor regions with the most aggressive growth characteristics, which would be optimal locations for biopsy. They investigated the ability to use one or more MR spectroscopic parameters to predict the MIB-1 cell proliferation index (PI), the terminal deoxynucleotidyl transferase–mediated deoxyuridine triphosphate nick-end labeling cell death index (DI), the cell density, and the ratio of proliferation to cell death (PI/DI) within different regions of the same tumor.

Methods. Patients with presumed Grades II or III glioma underwent 3D MR spectroscopic imaging prior to surgery, and two or three regions within the tumor were targeted for biopsy retrieval based on their spectroscopic features. Biopsy specimens were extracted from the tumor during image-guided resection, and the PI, DI, and cell density were assessed in the specimens using immunohistochemical methods.

Conclusions. The authors found that the relative levels of Cho and *N*-acetylaspartate (NAA) correlated with the cell density, PI, and PI/DI ratio within different regions of the same tumor and that the association held for the subpopulation of nonenhancing tumors. The association was stronger in tumors with large ranges of Cho/ NAA values, irrespective of the presence of contrast enhancement. The findings demonstrate the validity of using MR spectroscopy to identify regions of aggressive growth in presumed Grade II or III gliomas that would be suitable targets for retrieving diagnostic biopsy specimens.

Key Words • intratumoral heterogeneity • biopsy • magnetic resonance spectroscopy • MIB-1 index • TUNEL • glioma

Malignant gliomas represent the most common type of primary brain tumor, and astrocytomas constitute 75% of all gliomas. Oligodendrogliomas and mixed oligoastrocytomas account for roughly 9% and 11% of glial tumors, respectively.[2] The 5-year survival rates for patients in whom malignant glioma was diagnosed range from 36 to 68% for WHO Grade II glioma and 30 to 41% for Grade III glioma.[2] Grade II gliomas are characterized by increased nuclear atypia and cellularity as compared with normal parenchyma. For a tumor to be classified as Grade III, or anaplastic, mitotic figures must be observed in at least one of the biopsy specimens retrieved from the tumor for diagnostic purposes. Typically, Grade III gliomas also have a higher cell density than low-grade gliomas.[13]

The accurate diagnosis of Grade II or Grade III gliomas is crucial for the effective treatment of patients with these lesions. The extraction, during surgery, of a single biopsy specimen that shows mitotic activity is sufficient to upgrade a tumor from Grade II to Grade III. Gliomas are infiltrative and heterogeneous tumors that often have a mixture of histological features that are not apparent on MR imaging. Both grades of tumor may appear as nonenhancing or minimally enhancing lesions on T_1-weighted MR images. In such cases, there is no obvious area from which to extract a diagnostic biopsy specimen.

There can be dramatic differences in the postsurgical management of Grade II and Grade III tumors. Grade III gliomas are often treated aggressively with a combined regimen of chemotherapy and radiotherapy. Grade II gliomas, on the other hand, may be treated with chemotherapy alone, or patients with these tumors may not receive further treat-

Abbreviations used in this paper: CCI = Cho-to-creatine index; Cho = choline-containing compounds; CNI = Cho-to-*N*-acetylaspartate index; Cr = creatine and phosphocreatinine; DI = cell death index; FOV = field of view; LL = lactate and/or lipid; MR = magnetic resonance; NAA = *N*-acetylaspartate; PI = cell proliferation index; TUNEL = terminal deoxynucleotidyl transferase–mediated deoxyuridine triphosphate nick-end labeling; WHO = World Health Organization.

ment beyond surgical biopsy or resection until there is a suspicion of recurrence.

Recently, efforts have been made to improve the noninvasive diagnosis of glioma using advanced MR imaging methods. Of note are the results of recent studies that have demonstrated the potential for using MR spectroscopy to determine the histological grade and type of brain tumors.[5,7,9,14,15,22,25] The most common pattern observed in glioma compared with normal brain is an increase in the spectral peak corresponding to Cho.[4,6,17,19] Because the choline compounds measured with MR spectroscopy are associated with phospholipid metabolism,[20,21] the elevation of Cho levels is thought to reflect both an increase in cell density and proliferation. Typically, a decrease in the peaks corresponding to the neurotransmitter NAA and/or the metabolites Cr are also observed in conjunction with the increased Cho peak. Another MR spectroscopic pattern that has been observed primarily in high-grade gliomas is an elevation in the peak associated with LL,[10,12,17] which has been postulated to result from cell death processes, glucose consumption in proliferating tissue, and/or anaerobic metabolism in hypoxic tissue.

In the current study, instead of using the histological grade as the primary measure of tumor aggressiveness, we chose to investigate the metabolic features associated with tumor growth properties, specifically, proliferation, cell density, and apoptosis. We investigated the ability to predict the growth characteristics within different parts of the same tumor using one or more MR spectroscopic peaks. Such information would be useful in identifying aggressive regions within the tumor that would be optimal for extracting a biopsy specimen for diagnostic purposes. The purpose of these investigations was to determine whether MR spectroscopy could be used to direct biopsies of Grades II and III tumors.

Materials and Methods

Study Population

This study received full approval from the Committee on Human Research of the University of California, San Francisco. Our study population comprised 21 patients (11 women and 10 men) with untreated WHO Grade II (11 patients) or Grade III (10 patients) gliomas. With regard to tumor type, there were two oligodendrogliomas, five astrocytomas, four oligoastrocytomas, two anaplastic oligodendrogliomas, seven anaplastic astrocytomas, and one anaplastic oligoastrocytoma. Six of the Grade III lesions and one of the Grade II lesions exhibited contrast enhancement on T_1-weighted MR images.

Each patient underwent an MR imaging and spectroscopy examination 1 day prior to surgery. The MR spectroscopic data were aligned with the MR images and were used to identify three or four target regions within the hyperintense region on the T_2-weighted MR images for retrieving biopsy specimens. (The criteria for selecting the biopsy targets are outlined in the next section.) The MR images were mounted on the surgical navigation system (StealthStation, Medtronic), which provided the surgeon (M.S.B.) with a visual correlation between specific locations within the brain and locations on the MR images.

The biopsy specimens were obtained during open resection of the tumors. A prior study by the surgical team involved with this study showed that brain shifts as large as 6 mm can occur during resection and can result in a misregistration between the Stealth MR images and the patient's physical space.[11] The study also demonstrated that locations on the Stealth MR images could be coregistered with those on intraoperative ultrasonographic images to correct for postresection tissue shift with an error of less than 4 mm. Because the MR spectroscopic voxels measured 10 mm on each side, we always targeted the center of the voxel for biopsy specimen retrieval to allow for coregistration error.

Often a biopsy specimen could not be obtained from one or more of the target regions due to their being located in brain areas that controlled patient function or were inaccessible via surgery; nevertheless, at least two biopsy specimens were retrieved from each patient. In all, we retrieved 51 biopsy specimens: eight from oligodendrogliomas, 13 from astrocytomas, 12 from oligoastrocytomas, two from anaplastic oligodendrogliomas, and 16 from anaplastic astrocytomas. In two patients with Grade III tumors, we retrieved biopsy specimens that demonstrated Grade II histological characteristics. Immediately after retrieval, the biopsy specimens were fixed in 10% formalin and sent to the neuropathology service of the University of California, San Francisco, where they were embedded in paraffin and cut into sections for histopathological assessment.

Magnetic Resonance Imaging and Spectroscopy

Three-dimensional T_2-weighted and contrast-enhanced T_1-weighted MR images were obtained from each patient prior to surgery. The specific sequences were 3D fast spin echo (TR 3000 msec, TE 105 msec, matrix 256 × 256 × 114, voxel size 1.0 × 1.0 × 1.5 mm) and 3D spoiled gradient echo (TR 34 msec, TE 3 msec, flip angle 35°, matrix 256 × 256 × 124, voxel size 1.0 × 1.0 × 1.5 mm). The 3D sequences were necessary for accurate correspondence with anatomical locations during the surgery and the coregistration with the MR spectroscopic data that were acquired during the same examination. The MR spectroscopic imaging data that were acquired after the MR imaging was performed were also volumetric, although the resolution was coarser than that of the MR images. (Acquisition parameters: TR 1000 msec, TE 144 msec, matrix 12 × 12 × 8 or 16 × 16 × 8, FOV 120 × 120 × 80 mm or 160 × 160 × 80 mm, nominal voxel size 10 mm^3.) Specialized radiofrequency pulses were used to excite a 100- to 300-cm^3 volume that included most of the lesion area demonstrated on the T_2-weighted MR image and included normal-appearing parenchyma (Fig. 1). By using phase-encoding techniques similar to those used to acquire MR images, we divided the excited volume into 1-cm^3 voxels, each of which contained a single spectrum that characterized the metabolic activity in the underlying brain region.

The heights and areas of the resonance peaks corresponding to Cho at 3.2 ppm, Cr at 3.0 ppm, NAA at 2.0 ppm, and LL at 1.3 ppm were quantified at every voxel location in each examination. We also calculated relative Cho levels using two different methods: direct ratios of Cho to NAA and Cho to Cr, and a linear regression–based method that generates indices—the CNI and the CCI—reflecting the number of standard deviations of difference between the relative level of Cho in a given voxel and the mean relative level of Cho in voxels from nontumor regions.[12,14,18] The CNI and CCI were recently developed to generate more stable measures of Cho abnormality, particularly in voxels that have low NAA or Cr, which can drive the direct ratio to very large values, irrespective of the Cho level. We hypothesized that intratumoral differences in CNI values indicated differences in growth characteristics; therefore, we identified regions with high and low CNI values to target for biopsy specimen retrieval. Although four targets were routinely identified, in practice only two or three targets were located in noneloquent regions that were safe for biopsy.

After the biopsy specimens were collected, the saved images from the surgical navigation system were used as references for identifying the biopsy coordinates on the presurgical MR images. The coordinates were then used to reconstruct the MR spectrum that was centered at each biopsy location. On average, 65 voxels were selected from contralateral normal-appearing parenchymal regions in each patient and were used to generate four MR spectroscopic parameters at each biopsy site: the normalized Cho peak area, the normalized Cr peak area, normalized NAA peak area, and a binary score indicating the presence or absence of a peak in the LL region.

The resonance peaks in the LL region of the spectra were typically either completely absent or high enough to be visually distinguished from the noise but not always with sufficient signal to be accurately quantified. In an attempt to quantify this observation, we calculated the signal-to-noise ratio for the LL peak areas and found

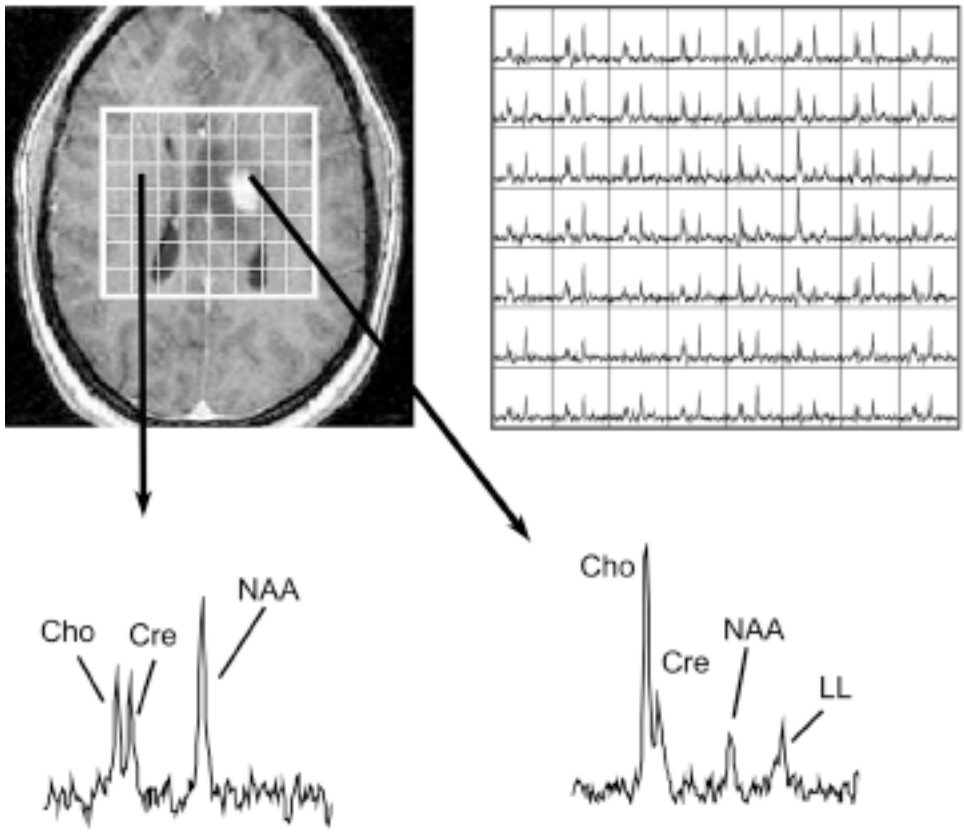

FIG. 1. Contrast-enhanced T_1-weighted MR image and corresponding MR spectroscopic array *(upper)* obtained in a patient with a Grade III astrocytoma. The spectrum from the enhancing tumor *(lower right)* shows elevated peaks corresponding to Cho and LL and decreased peaks corresponding to Cr (Cre) and NAA relative to the spectrum from contralateral healthy-appearing brain *(lower left)*.

that those peaks with a signal-to-noise ratio of 6 or lower were most often visually indistinguishable from noise. Based on these empirical observations, the LL value was assigned a 1 (present) if the signal-to-noise ratio was greater than 6 or assigned a 0 (absent) if it fell below the signal-to-noise ratio threshold. We verified all LL assignments by reviewing the actual spectra.

Immunohistochemical Analysis

To obtain a measure of the cellular proliferation and death rates of the biopsy specimens, immunoperoxidase MIB-1 and immunofluorescence TUNEL assays were performed on the 51 tissue specimens. Two 5-μm sections were taken from each biopsy and baked onto glass slides at 70°C, then dewaxed with xylenes and rehydrated by incubation in a graded series of solutions of ethanol (100–50%) and phosphate-buffered saline. The specimens were then incubated in 0.025% trypsin and microwaved in citrate buffer (10 mM, pH 6.0) to increase antigen and end-labeling sensitivity. The samples that were assayed for MIB-1 reactivity were incubated in 3.0% H_2O_2 in phosphate-buffered saline to inactivate the endogenous peroxidases. Nonspecific antibody binding was blocked by incubating samples in a solution of 10% normal horse serum prior to incubating overnight with MIB-1 antibody (Dako, Denmark) diluted 1:500 in 10% normal horse serum. The MIB-1 binding was amplified with a biotinylated secondary antibody bound to an avidin-biotin-horseradish peroxidase complex (Vectstain Elite ABC kit, Vector Laboratories) and detected with diaminobenzidine tetrachloride (DAB, Vector Laboratories). The cells were then counterstained with hematoxylin to obtain a measure of cell density. The immunoperoxidase procedure resulted in high nonspecific background staining when we used it for the TUNEL assay; therefore, we chose to use immunofluorescence detection instead. On samples assayed with TUNEL, we used an In Situ Cell Death Detection kit (Roche Diagnostics) to end-label DNA strand breaks with fluorescein following the citrate buffer permeabilization step. The cells were then visualized using a fluorescence microscope.

A count of 1000 cells was performed on each hematoxylin-stained slide using 0.2-mm^2 FOVs at a magnification of 20. The MIB-1 PI was determined by dividing the number of MIB-1–labeled cells by the total number of cells within each FOV. The cell density was determined by dividing the total number of cells counted on each slide by the number of fields. The DI was determined by dividing the average number of TUNEL-labeled cells by the cell density of the sister slide that was subjected to MIB-1 and hematoxylin staining. Care was taken to ensure that counts were performed on the same number of FOVs for both the PI and DI assessments. Lastly, a measure of net growth rate was calculated by dividing the PI by the DI.

Statistical Analysis

The SPSS statistical software package (SPSS, Inc.) was used for all analyses. To evaluate the ability to use one or a combination of the MR spectroscopic parameters to predict the growth characteristics of specific regions within a tumor, we first ranked the four immunohistochemical parameters (cell density, PI, DI, and the PI/DI ratio) and three of the MR spectroscopic parameters (the normalized peak areas for Cho, Cr, and NAA) by patient. To preserve the binary information, the LL values were not ranked. We used a univariate linear model of each pair of MR spectroscopic and immunohistochemical variables to determine whether a single MR spectroscopic measure (independent variable) predicted any of the growth measures (dependent variables). We then determined whether the combined MR spectroscopic parameters predicted any of the immunohistochemical values using a multivariate linear model in which all four MR spectroscopic parameters were independent variables. To further investi-

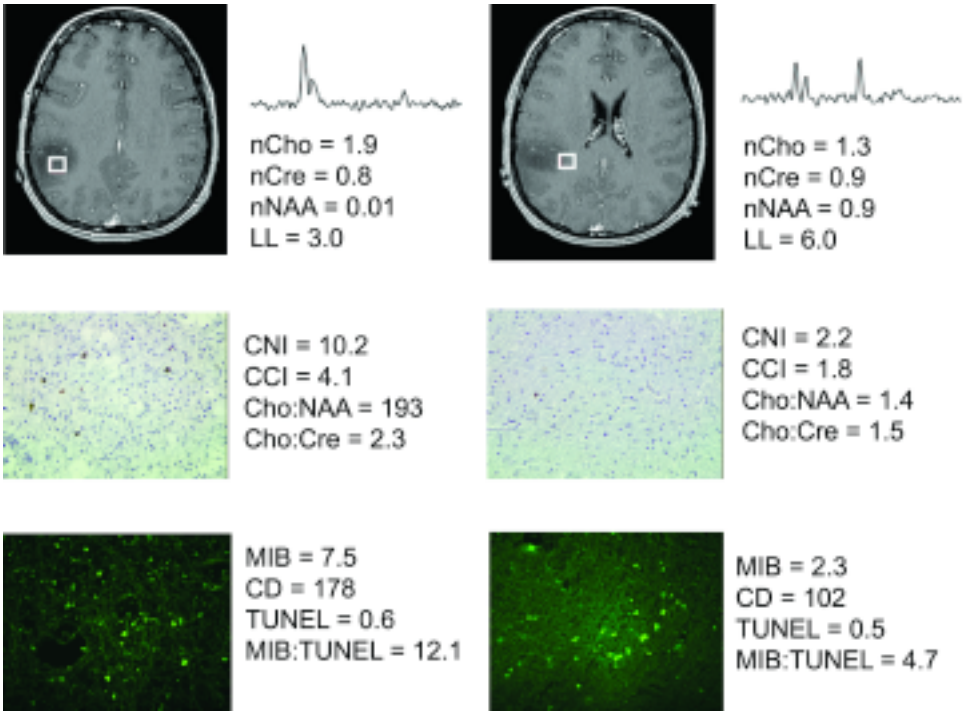

FIG. 2. Magnetic resonance spectroscopic and immunohistochemical data corresponding to two different biopsies obtained in a patient harboring a Grade III astrocytoma. MIB-1 *(center)* and TUNEL *(lower)*. Orginial magnifications × 200. CD = cell density; nCho = normalized Cho; nCre = normalized Cr; nNAA = normalized NAA.

gate the predictive capabilities of combined MR spectroscopic measures involving Cho, we ranked the Cho/NAA ratio, Cho/Cr ratio, CNI, and CCI by patient and again performed a univariate regression. The analyses were repeated on data from three subgroups: Grade II tumors (11 tumors), Grade III tumors (10 tumors), and nonenhancing tumors (14 tumors). In interpreting the results of our analyses, it is important to take into account the issue of multiple comparisons. For the purpose of highlighting potentially interesting results, correlations were declared to be statistically significant if the probability value was 0.025 or less. Although this value is lower than the usual alpha level of 0.05, it does not fully adjust for the number of comparisons. We did not want to reduce the power of the study by requiring too stringent a criterion for declaring significance.

Results

Figure 2 shows an example of two biopsy specimens obtained from the same nonenhancing tumor that had very different MR spectroscopic profiles and growth characteristics. Although one specimen had significantly higher PI and cell density than the other, both were determined to represent Grade III astrocytoma.

We ranked the data within each patient and modeled the relationship between the immunohistochemical and MR spectroscopic values as a linear regression so that the slope would tell us the direction of the association and the probability value would reflect the strength of the association. No single independent MR spectroscopic parameter exhibited a significant relationship with any of the immunohistochemical parameters (data not shown). Similarly, when we modeled the data using the combined MR spectroscopic parameters as independent variables, we did not find a linear relationship with any of the growth measures.

We further investigated the relationship between multiple MR spectroscopic measures and each immunohistochemistry measure using Cho ratios (Cho/NAA and Cho/Cr) and indices (CNI and CCI). Table 1 shows the slopes of the univariate regressions for each pair of parameters. Significant correlations were found between the Cho/NAA ratio and cell density ($p < 0.001$), PI ($p < 0.001$), and the PI/DI ratio ($p = 0.003$). All of the correlations were positively directed. We also found that the cell density ($p = 0.025$), PI ($p = 0.013$), and PI/DI ratio ($p = 0.005$) increased as the CNI increased. There was a trend toward increasing CCI with increasing DI, but it did not reach statistical significance ($p = 0.069$). Thus, the relative levels of Cho and NAA, as measured by either the ratio or the index, appeared to be the strongest indicator of net and cumulative growth within the tumor.

To confirm that the associations found among all patients were consistent within the tumor subgroups, we performed independent analyses on the Grade II gliomas (11 tumors), the Grade III gliomas (10 tumors), and the nonenhancing tumors (14 tumors). The data are shown in Table 2. When considered on their own, the Grade II tumors did not exhibit any of the relationships observed in the overall data. However, the CNI and Cho/NAA ratio in the Grade III tumors predicted the cell density, PI, and PI/DI values, just as we observed in the full cohort of patients. The subgroup of nonenhancing tumors exhibited all but two of the associations seen in the overall group. Specifically, the Cho/NAA ratio increased with cell density, PI, and PI/DI, whereas the CNI increased with cell density only. There was a trend toward increasing PI/DI with increasing CNI ($p = 0.035$) in the nonenhancing tumors, but it did not reach statistical significance. Taken together, these results suggest that targeting the region with the highest Cho/NAA in nonenhancing tu-

TABLE 1

Slopes and probability values from univariate regression analysis of within-patient Cho parameters and growth indices

Growth Index	Cho/NAA		Cho/Cr		CNI		CCI	
	Slope	p Value	Slope	p Value	Slope	p Value	Slope	p Value
cell density	0.51*	<0.001	0.12	0.408	0.31*	0.025	0.00	0.977
PI	0.48*	<0.001	0.15	0.290	0.35*	0.013	0.24	0.097
DI	0.15	0.332	0.18	0.231	0.19	0.208	0.27	0.069
PI/DI	0.43*	0.003	0.20	0.193	0.41*	0.005	0.22	0.146

* Statistically significant at $p \leq 0.025$.

mors may improve the probability of finding a region of high cell density, high proliferative fraction, and/or high ratio of cell proliferation to cell death. The assertion holds for Grade III tumors, whether or not they demonstrate enhancement on MR images, but Grade II tumors may not exhibit such relationships.

To evaluate whether the lack of correlation within the Grade II tumors was due to a small range of values for the immunohistochemical and/or MR spectroscopic data compared with the Grade III tumors, we compared the difference between the intratumoral minimum and maximum values for both groups. The 10th, 25th, 50th, 75th, and 90th percentiles for the intratumoral range of values within each grade are shown in Table 3. Indeed, the Grade III tumors appeared to be more heterogeneous than the Grade II tumors with respect to cell density, PI, CNI, and Cho/NAA as illustrated by the 50th, 75th, and 90th percentiles for those measures. Table 3 also shows that the ranges of values for cell density, CNI, and the Cho/NAA ratio in the nonenhancing tumors (10 Grade II and four Grade III lesions) fall somewhere in between the values for the Grade II and III tumors, although they exhibited relationships between the MR spectroscopic and growth measures at rates similar to that of the Grade III tumors. Taken together, these results suggest that tumor heterogeneity may influence the detection of abnormal growth activity by MR spectroscopy and that the range of growth measures in the Grade II tumors may not have been large enough to result in a sufficient range of intratumoral CNIs or Cho/NAA ratios for an association to occur.

Discussion

To our knowledge, this is the first demonstration that MR spectroscopy can be used to assess growth properties within different regions within the same glial tumor. Specifically, we found that the relative levels of Cho and NAA correlated with the degree of cell density, PI, and PI/ DI ratio within different regions of the same tumor. We also demonstrated that the relationship between the MR spectroscopic and growth measures held for nonenhancing tumors. The association was stronger in the more heterogeneous tumors and did not hold for the more homogeneous tumors. These results suggest that tumors with "hot spots" of high levels of Cho relative to NAA are likely to have "hot spots" of growth activity occurring in the same location, even if they do not exhibit enhancement with contrast administration on MR images. Such information is extremely useful for guiding diagnostic biopsies of presumed Grade II or III gliomas.

It is generally accepted that both the Cho/NAA and Cho/Cr ratios increase with the histological grade of gliomas, but reports differ as to which ratio is the better predictor of tumor aggressiveness,[7,10,14,23,24] possibly because of the different MR spectroscopic acquisition methods used in the various studies. A major difficulty of using ratios as quantitative measures of abnormality is that they become unstable in regions of low signal, such as near the lateral ventricles, where both the numerator and the denominator become very small. In an attempt to circumvent this problem, we developed a method for quantifying the relative sizes of metabolic peaks that is less sensitive to tissue content and is normalized by the relative peak sizes in presumed healthy regions of the brain of the individual undergoing the study.[14,18] The two indices—CNI and CCI—that result from our method were tested along with the respective ratios in the current study to determine which measures were most closely associated with the tumor growth parameters. The lower probability values of the associations with the Cho/NAA ratio as compared with those of the CNI suggest that the Cho/NAA ratio may be more sensitive to differences in

TABLE 2

Slopes and probability values from univariate regression analysis of tumor subgroups

Glioma Subgroup	CNI vs						Cho/NAA vs					
	Cell Density		PI		PI/DI		Cell Density		PI		PI/DI	
	Slope	p Value	Slope	p Value	Slope	p Value	Slope	p Value	Slope	p Value	Slope	p Value
Grade II	0.05	0.822	0.18	0.364	0.28	0.179	0.32	0.106	0.18	0.364	0.21	0.320
Grade III	0.56*	0.004	0.50*	0.013	0.52*	0.013	0.69*	0.000	0.75*	0.000	0.62*	0.002
nonenhancing	0.39*	0.022	0.23	0.196	0.39	0.035	0.45*	0.008	0.45*	0.008	0.42*	0.019

* Statistically significant at $p \leq 0.025$.

TABLE 3

*Distribution of the intratumoral ranges (maximum − minimum) of MR spectroscopic and immunohistochemical values for tumor subgroups**

	Cell Density Range			PI Range			PI/DI Range			CNI Range			Cho/NAA Range		
Percentile	Gr II	Gr III	NE	Gr II	Gr III	NE	Gr II	Gr III	NE	Gr II	Gr III	NE	Gr II	Gr III	NE
10th	33	27	35	0.5	0.3	0.6	12	7	8	0.3	0.2	0.3	0.8	1.4	0.8
25th	69	50	69	1.2	1.3	1.2	16	12	15	0.4	0.5	0.4	1.0	1.8	1.0
50th	85	103	85	3.6	3.2	2.7	47	38	34	1.0	2.7	1.0	1.4	6.2	1.4
75th	156	139	140	6.1	8.9	5.7	132	89	104	3.1	7.8	3.5	3.6	18.0	7.8
90th	177	195	190	8.4	14.1	7.6	689	525	635	4.1	11.7	7.9	191	176	124

* Gr II = Grade II glioma; Gr III = Grade III glioma; NE = nonenhancing glioma.

the growth measures than the CNI. As we stated earlier, however, such large ratios can occur in regions of low signal which may or may not correspond to aggressive tumor; in other words, the specificity of the Cho/NAA ratio is low. For this reason, the best criterion for choosing an appropriate biopsy target would be that both the Cho/NAA and CNI in a particular region are near the maximum values. In addition, based on our findings regarding heterogeneity, the maximum values should be substantially higher than the values in most of the tumor for the MR spectroscopic findings to be a useful indicator of growth activity. The distribution of intratumoral value ranges in Table 3 can be used as a guide for deciding if there is a sufficient range of Cho/NAA values in a given tumor to warrant using them to target diagnostic biopsies.

A significant finding of this study was that the ratio of Cho to NAA levels, and not the ratio of Cho to Cr levels, predicted growth properties in different regions of the same tumor. Reports differ as to which pair of MR spectroscopic resonances is the better indicator of proliferation and cell density in brain tumors, with substantial evidence being reported for both.[1,3,8,16] Our results suggest that, within any given tumor, the NAA level may better reflect the cell density and proliferative status whereas the Cr level may be more indicative of the apoptotic fraction (CCI compared with DI, Table 1). Thus the predominant mechanism of growth—increased proliferation or decreased cell death—for a specific tumor or tumor region may determine the MR spectroscopic pattern that is observed. Because the relationship between CCI and DI in this study was only a trend, however, more studies are necessary to validate this assertion.

Conclusions

The results of the intratumoral analysis provide biological evidence for considering the relative levels of Cho and NAA (Cho/NAA ratio) when deciding where to retrieve diagnostic biopsy specimens from tumors that have the classic imaging features of WHO Grade II or Grade III gliomas. Although the predictive capability of MR spectroscopy can vary in individual patients, we have provided initial evidence that the range of MR spectroscopic values observed within the tumor may be indicative of how well the relative Cho and NAA levels track with the local growth characteristics. These findings demonstrate the potential clinical utility of using multivoxel MR spectroscopy in the diagnostic assessment of patients with presumed Grades II or III gliomas.

Acknowledgments

We thank Terry Le, B.S., for her assistance in the preparation of this manuscript and Andrea Pirzkall, M.D., for her expert contributions to the study.

References

1. Barbarella G, Ricci R, Pirini G, Tugnoli V, Tosi MR, Bertoluzza A, et al: In vivo single voxel 1H MRS of glial brain tumors: correlation with tissue histology and in vitro MRS. **Int J Oncol 12:**461–468, 1998
2. CBTRUS: **Statistical Report: Primary Brain Tumors in the United States, 1998–2002.** Hinsdale, IL: CBTRUS, 2002
3. Croteau D, Scarpace L, Hearshen D, Gutierrez J, Fisher JL, Rock JP, et al: Correlation between magnetic resonance spectroscopy imaging and image-guided biopsies: semiquantitative and qualitative histopathological analyses of patients with untreated glioma. **Neurosurgery 49:**823–829, 2001
4. Falini A, Calabrese G, Origgi D, Lipari S, Triulzi F, Losa M, et al: Proton magnetic resonance spectroscopy and intracranial tumors: clinical perspectives. **J Neurol 243:**706–714, 1996
5. Fountas KN, Kapsalaki EZ, Gotsis SD, Kapsalakis JZ, Smisson HF III, Johnston KW, et al: In vivo proton magnetic resonance spectroscopy of brain tumors. **Stereotact Funct Neurosurg 74:**83–94, 2000
6. Fulham MJ, Bizzi A, Dietz MJ, Shih HH, Raman R, Sobering GS, et al: Mapping of brain tumor metabolites with proton MR spectroscopic imaging: clinical relevance. **Radiology 185:**675–686, 1992
7. Furuya S, Naruse S, Ide M, Morishita H, Kizu O, Ueda S, et al: Evaluation of metabolic heterogeneity in brain tumors using 1H-chemical shift imaging method. **NMR Biomed 10:**25–30, 1997
8. Gupta RK, Cloughesy TF, Sinha U, Garakian J, Lazareff J, Rubino G, et al: Relationships between choline magnetic resonance spectroscopy, apparent diffusion coefficient and quantitative histopathology in human glioma. **J Neurooncol 50:** 215–226, 2000
9. Hagberg G: From magnetic resonance spectroscopy to classification of tumors. A review of pattern recognition methods. **NMR Biomed 11:**148–156, 1998
10. Howe FA, Barton SJ, Cudlip SA, Stubbs M, Saunders DE, Murphy M, et al: Metabolic profiles of human brain tumors using quantitative in vivo 1H magnetic resonance spectroscopy. **Magn Reson Med 49:**223–232, 2003
11. Keles GE, Lamborn KR, Berger MS: Coregistration accuracy and detection of brain shift using intraoperative sononavigation during resection of hemispheric tumors. **Neurosurgery 53:** 556–564, 2003
12. Li X, Lu Y, Pirzkall A, McKnight T, Nelson SJ: Analysis of the spatial characteristics of metabolic abnormalities in newly diagnosed glioma patients. **J Magn Reson Imaging 16:**229–237, 2002

13. Lopes MBS, Vandenberg SR, Scheithauer BW: Histopathology, immunochemistry, and ultrastructure of brain tumors, in Kaye AH, Laws ER (eds): **Brain Tumors: An Encyclopedic Approach.** Edinburgh: Churchill Livingstone, 1995, pp 125–162
14. McKnight TR, Noworolski SM, Vigneron DB, Nelson SJ: An automated technique for the quantitative assessment of 3D-MRSI data from patients with glioma. **J Magn Reson Imaging 13:**167–177, 2001
15. Meyerand ME, Pipas JM, Mamourian A, Tosteson TD, Dunn JF: Classification of biopsy-confirmed brain tumors using single-voxel MR spectroscopy. **AJNR Am J Neuroradiol 20:** 117–123, 1999
16. Nafe R, Herminghaus S, Raab P, Wagner S, Pilatus U, Schlote W, et al: Correlation between preoperative magnetic resonance spectroscopic data on high grade gliomas and morphology of Ki-67-positive tumor cell nuclei. **Anal Quant Cytol Histol 25:** 131–138, 2003
17. Negendank WG, Sauter R, Brown TR, Evelhoch JL, Falini A, Gotsis ED, et al: Proton magnetic resonance spectroscopy in patients with glial tumors: a multicenter study. **J Neurosurg 84:**449–458, 1996
18. Nelson SJ: Analysis of volume MRI and MR spectroscopic imaging data for the evaluation of patients with brain tumors. **Magn Reson Med 46:**228–239, 2001
19. Nelson SJ, McKnight TR, Henry RG: Characterization of untreated gliomas by magnetic resonance spectroscopic imaging. **Neuroimag Clin N Am 12:**599–613, 2002
20. Nishizuka Y: Membrane phospholipid degradation and protein kinase C for cell signalling. **Neurosci Res 15:**3–5, 1992
21. Podo F: Tumour phospholipid metabolism. **NMR Biomed 12:** 413–439, 1999
22. Preul MC, Caramanos Z, Collins DL, Villemure JG, Leblanc R, Olivier A, et al: Accurate, noninvasive diagnosis of human brain tumors by using proton magnetic resonance spectroscopy. **Nat Med 2:**323–325, 1996
23. Shimizu H, Kumabe T, Tominaga T, Kayama T, Hara K, Ono Y, et al: Noninvasive evaluation of malignancy of brain tumors with proton MR spectroscopy. **AJNR Am J Neuroradiol 17:** 737–747, 1996
24. Tate AR, Majos C, Moreno A, Howe FA, Griffiths JR, Arus C: Automated classification of short echo time in in vivo 1H brain tumor spectra: a multicenter study. **Magn Reson Med 49:**29–36, 2003
25. Underwood J, Tate AR, Luckin R, Majos C, Capdevila A, Howe F, et al: A prototype decision support system for MR spectroscopy-assisted diagnosis of brain tumors. **Medinfo 10:**561–565, 2001

Manuscript submitted December 29, 2005.
Accepted August 18, 2006.
This work was supported by National Institutes of Health Grants No. K01-CA90244 to Dr. McKnight, No. R01-CA79719 to Drs. Nelson and Lamborn, and No. P50-CA097257 to Drs. Berger, Chang, and Lamborn.

Address reprint requests to: Tracy McKnight, Ph.D., 185 Berry Street, Suite 350, Center for Molecular and Functional Imaging, University of California, San Francisco, California 94107. email: mcknight@mrsc.ucsf.edu.